DVS Application Note 39

Measuring Moisture Sorption and Diffusion Kinetics on Proton Exchange Membranes Using the DVS

Dan Burnett, Armando R. Garcia, and Frank Thielmann, Surface Measurement Systems Ltd.

Dynamic Vapour Sorption (DVS) allows the fast and accurate determination of water sorption isotherms and diffusion kinetics over a wide temperature and humidity range. This paper describes the water sorption behaviour on three Nafion® based fuel cell membranes.

Introduction

Proton Exchange Membrane Fuel Cells (PEMFC) are an expanding area of research for use as low pollution power generators for mobile and stationary applications. The PEMFC is composed of a membrane electrode assembly consisting of several layers. There are typically two carbon cloth gas-diffusion layers that allow concurrent transport of gases and water while collecting current and two carbon-supported Pt based catalyst layers where the electrochemical reactions take places. These layers are sandwiched between a proton exchange membrane that permits proton transfer from anode to cathode [1].

A critical parameter affecting the performance of these proton exchange membranes is the water content. Water is supplied to the fuel cell by humidifying the gas feed stream. The level of hydration within the proton exchange membrane is vital to its performance. If the hydration level is too low, the polymers exhibit greatly reduced ionic conductivity [2]. Membrane dehydration is a well-known fuel cell failure mechanism. On the other side of the spectrum, if hydration level is too high, excess water can flood the pores in the gas diffusion layer and block off reaction sites or

impede mass transport within the electrode structure [3,4]. In addition, the water vapour diffusion coefficients as a function of water content are important parameters in characterizing the performance of proton exchange membranes [4].

Related to the water content is the operating temperature of the proton exchange membrane. Increasing the operating temperature above room temperature improves the electrode kinetics of the oxygen reduction reaction [5]. However, if the temperature is above the boiling point of water, the water content in the polymer decreases leading to a decrease in conductivity [6]. Additionally, if the temperature is above the glass transition for the polymer, then polymer chain rearrangement can occur and cause structural changes in the membrane, lower membrane stability, and reduce performance [5]. For the above reasons, it is important to study the behaviour of these films over a wide temperature and humidity ranges.

In this application note, the water content and diffusion kinetics were studied on three different Nafion® based membranes over a range of temperatures. Nafion® is a commercially available perfluorosulfonic acid polymer often used as an exchange membrane in PEMFC's. Nafion® is an ideal choice for PEMFC

applications due to its high chemical and electrochemical stability, sufficient mechanical strength, low permeability to reactant species, selective and high ionic conductivity, and electronic insulation properties [7]. Nafion® has further applications as a novel clothing materials for protection from chemical warfare agents, separators in chloro-alkali cells, and as super acid catalysts [8,9]. For the above reasons, Nafion® films were used in this application note as model proton exchange membranes.

Method

Dynamic gravimetric vapour sorption (DVS) is a well-established method for the determination of vapour sorption isotherms. The DVS Advantage-1 instrument used for these studies measures the uptake and loss of vapour gravimetrically using a SMS UltraBalance with a mass resolution of ±0.1 μg. The high mass resolution and excellent baseline stability allow the instrument to measure the adsorption and desorption of very small amounts of probe molecule. The vapour partial pressure around the sample is controlled by mixing saturated and dry carrier gas streams using electronic mass flow controllers. The temperature is maintained constant ±0.1 °C, by enclosing the entire system in a temperature-controlled incubator.

For the DVS experiments, a small (~ 1 cm^2) section of film was placed in a stainless steel mesh sample pan. The 400 mesh pan (400 lines per inch) allowed direct vapour flow to all sides of the film. The sample pan was then placed in the DVS at the desired temperature and dried at 0% RH to establish a dry mass. After a stable, dry mass was achieved, the sample was exposed to the following humidity profile: 0% RH, 30% RH, 60% RH, 90% RH, 60% RH, 30% RH, and 0% RH. Mass equilibrium was reached at each humidity stage by measuring the percentage change in mass with respect to time (i.e. slope or dm/dt). Once the mass slope was below a predetermined threshold value and equilibrium was achieved; the experiment proceeded to the next programmed humidity stage. For some

experiments a second complete sorption and desorption cycle was collected to investigate any irreversible changes or sample history effects. Complete sorption and desorption isotherms were collected at 30, 50, and 70 °C. A new sample was used for each temperature to minimize any thermal history effects.

From the initial vapour uptakes with each change in relative humidity, it is possible to calculate the water vapour diffusion constant into the film. This approach to diffusion constant determination via DVS is explained in detail in SMS Application Note 16 [10]. In short, a thin film sample, with thickness d, is placed in the DVS and for a single step change in humidity the initial kinetics of sorption into the bulk for a two-sided film may be described by Equation 1 below:

$$\frac{M_t}{M_\infty} = \frac{4}{d}\sqrt{\frac{Dt}{\pi}} \qquad (1)$$

where M_t is the amount adsorbed at time t, M_∞ is the amount adsorbed at thermodynamic equilibrium, and D is the diffusion constant. This equation is applied for values of M_t/M_∞ <0.4, where a plot of M_t/M_∞ against $t^{1/2}/d$ should be linear. The diffusion constant D can then be calculated from the slope of this line. The only input parameter necessary for these calculations is the film thickness. Diffusion constants were calculated for each step change in humidity at each temperature. In order to monitor fast diffusion processes, data points were collected every 2 seconds for these experiments. For the linear fit described above, a minimum R-squared value of 99.9% was used for all diffusion calculations.

Three different Nafion® films were obtained from Dupont: N-117, N-112, and NR-112. All three films are based on the Nafion® material, which is a perfluorosulfonic acid/TFE copolymer in the acid (H$^+$) form. N-117 and N-112 are non-reinforced extruded films while the NR-112 material is a non-reinforced dispersion-cast film. The N-117 sample is 183 microns thick at 23 °C and 50% RH, while the N-112 and NR-112 samples are 51 microns thick at the same conditions. These film

thickness values were used for all diffusion calculations. The effect of film thickness for the same base material can be investigated by comparing the results from the N-117 and N-112 samples, while the effect of extruded or dispersion-cast films can be studied by comparing the N-112 and NR-112 samples.

Results

Figure 1 displays the typical moisture sorption and desorption kinetic results obtained from the three samples. Specifically, Figure 1 shows the moisture sorption and desorption results for the N-117 sample at 30 °C. Two complete sorption and desorption cycles were collected. The red trace displays the percentage change in mass, referenced to the dry mass, versus time on the left axis while the blue trace shows the chamber RH as a function of time on the right axis. The sample mass increases or decreases with each increase or decrease in humidity and rapidly reaches equilibrium. From these equilibrium points the isotherm can be determined. Figure 2 displays the water vapour isotherm for this N-117 sample at 30 °C. The first cycle is shown in red (sorption) and blue (desorption), while the second cycle is represented by the green (sorption) and pink (desorption) traces. Notice, for this particular sample and conditions there is virtually no difference between the first and second cycle isotherms. Also, there is little to no hysteresis between the sorption and desorption isotherms. Together, these results indicate that water sorption is completely reversible and there are no sample history effects related to water sorption.
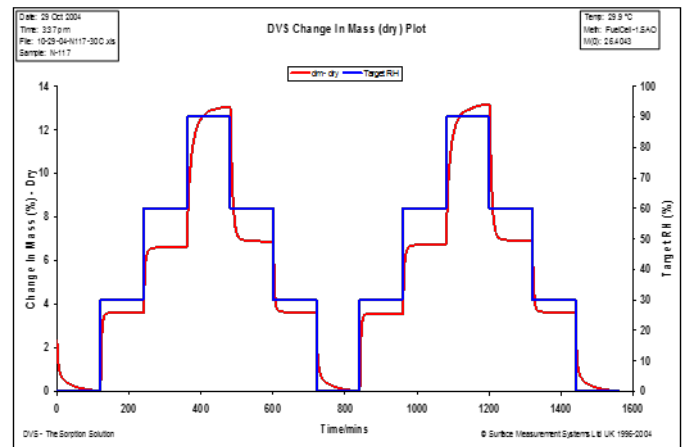

Figure 1. Moisture sorption and desorption kinetics for the N-117 sample at 30 °C.
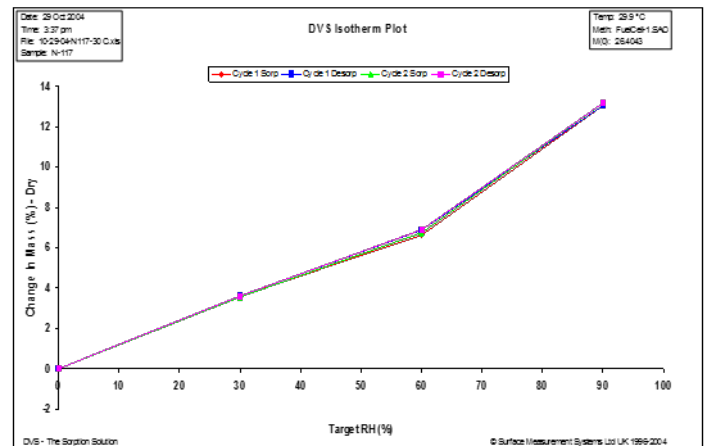

Figure 2. Moisture sorption and desorption isotherms for the N-117 sample at 30 °C.

Identical experiments were performed for all three samples at 30, 50, and 70 °C. Figure 3 shows the first cycle sorption (solid lines) and desorption (dashed lines) isotherm results for the N-117 (red), N-112 (blue), and NR-112 (green) samples at 30 °C (a.), 50 °C (b.), and 70 °C (c.). Note, only the first cycle isotherms are shown for each sample, because the second cycle isotherms were nearly identical to the first cycle, indicating a completely reversible water vapour sorption/desorption mechanism. The differences between samples are greatest at 30 °C (Figure 3a), where the percentage water uptake shows the following trend: N-112 > NR-112 > N-117. In comparing the two extruded samples, the results at 30 °C indicate that the thinner N-112 sample is able to uptake a greater percentage (based on
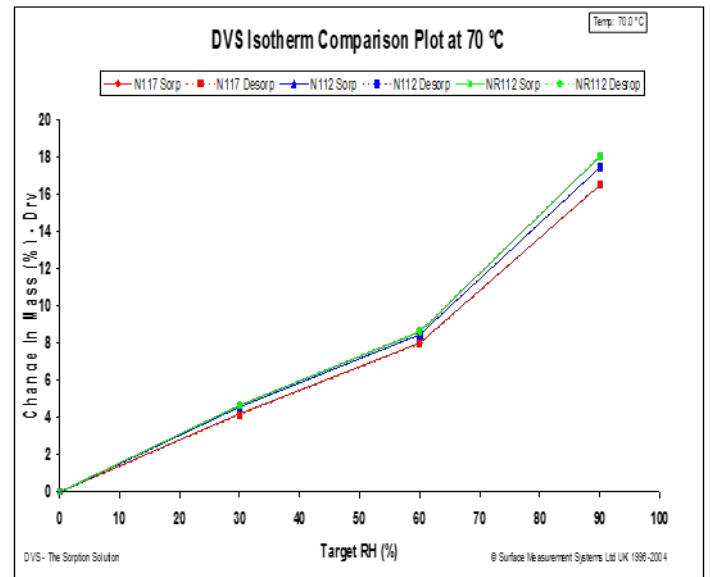
weight) than the thicker N-117 sample. The thicker sample may impede water diffusing throughout the entire film, resulting in the lower water uptake. The extruded N-112 sample has a slightly higher water uptake than the dispersion-cast NR-112 sample at 30 °C, suggesting the extruded sample may allow improved water diffusion into the bulk.
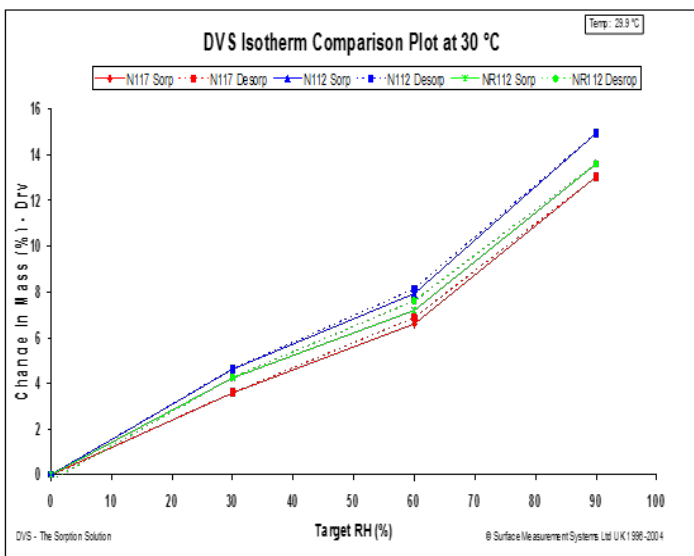

(a.)
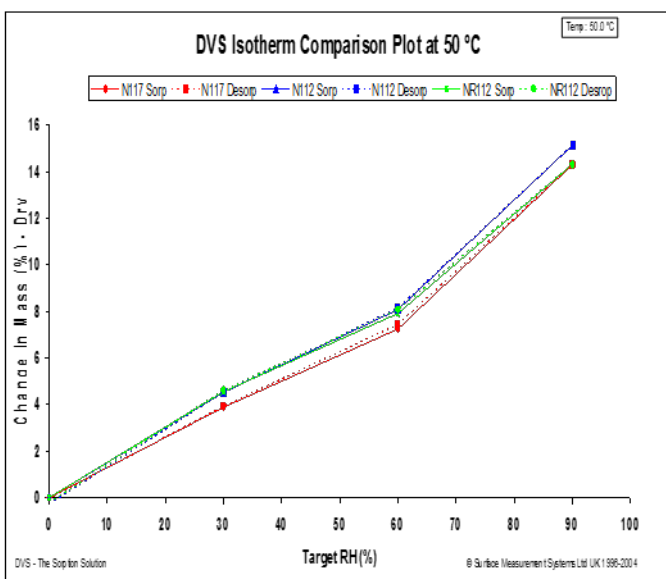
(b.)

(c.)

Figure 3. First cycle sorption (solid lines) and desorption (dashed lines) isotherm comparisons between the N-117 (red), N-112 (blue), and NR-112 (green) samples at 30 °C (a.), 50 °C (b.), and 70 °C (c.).

At higher temperatures, the differences are much smaller and approaching the error margins of the experiment. The differences between the thicker (N-117) and thinner (N-112) samples observed at 30 °C may be minimized at 50 and 70 °C due to the increased molecular mobility at the higher temperatures. The increased molecular mobility at higher temperatures may increase water diffusion, thus allowing water to access more of the sample.
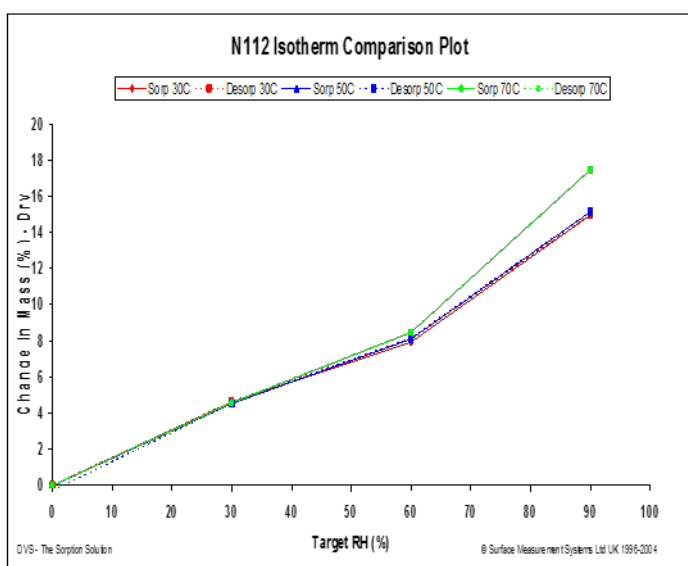
Figure 4 compares the isotherms for the N-117 (a.), N-112 (b.), and NR-112 (c.) samples as a function of temperature. The isotherm at 30 °C is in red, 50 °C in blue, and 70 °C is in green.

(a.)

(c.)
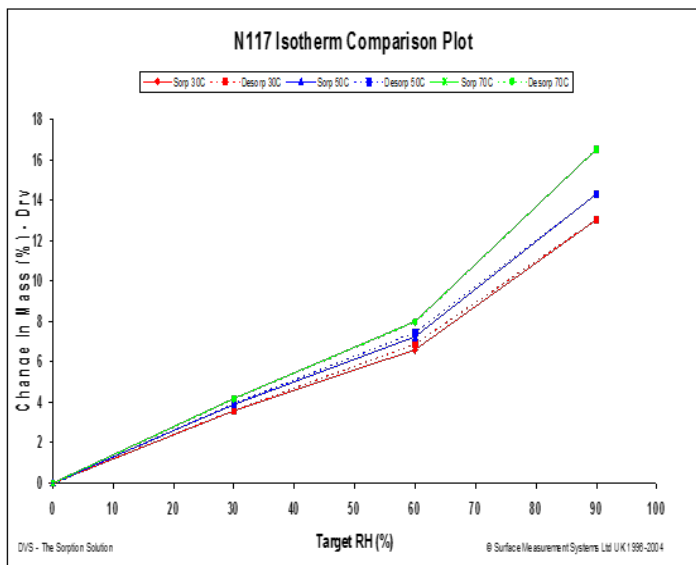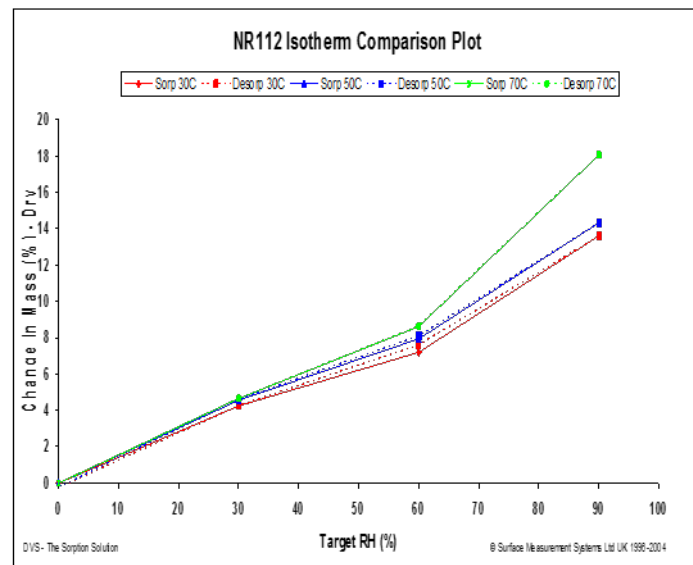
Figure 4. Isotherm comparisons for the N-117 (a.), N-112 (b.), and NR-112 (c.) samples at 30 ° C (red), 50 °C (blue), and 70 °C (green).

(b.)

For each sample, there is an increase in percentage weight gain of water vapour with increasing temperature. As hypothesized above, the higher temperatures will increase molecular mobility within the samples and allow for more water to diffuse and absorb into the bulk structure of the films. The hysteresis gaps between sorption and desorption isotherms support this trend. There is a small, but measurable hysteresis at 30 °C for all samples. However, this gap decreases with increasing temperature and is non-existent at 70 °C. The smaller hysteresis gaps at higher temperatures indicate the water sorption is not diffusion limited. This may also be supported when comparing the diffusion coefficient data discussed below.

The diffusion constants were calculated for each step change in humidity as described in the experimental section. Table 1 lists the diffusion constants and R-squared values for the N-117 (a.), N-112 (b.) and NR-112 (c.) samples at 30 °C, 50 °C, and 70 °C.

Table 1a. Diffusion coefficient values for the N-117 sample.

Previous RH%	Target RH%	30 °C		50 °C		70 °C	
		Diffusion Coeff.	R-sq.(%)	Diffusion Coeff.	R-sq.(%)	Diffusion Coeff.	R-sq.(%)
0.0	30.0	2.38E-07	99.03	6.37E-07	99.07	1.02E-06	99.06
30.0	60.0	3.03E-07	99.19	5.58E-07	99.27	9.86E-07	99.31
60.0	90.0	6.35E-08	99.11	1.07E-07	99.05	6.46E-07	99.11
90.0	60.0	1.08E-07	99.11	1.86E-07	99.10	7.34E-07	99.24
60.0	30.0	2.76E-07	99.20	6.65E-07	99.05	1.80E-06	99.19
30.0	0.0	2.27E-07	99.19	6.36E-07	99.12	1.22E-06	99.05

Table 1b. Diffusion coefficient values for the N-112 sample.

Previous RH%	Target RH%	30 °C		50 °C		70 °C	
		Diffusion Coeff. (cm²/s)	R-sq. (%)	Diffusion Coeff. (cm²/s)	R-sq. (%)	Diffusion Coeff. (cm²/s)	R-sq. (%)
0.0	30.0	1.17E-07	99.07	3.60E-07	99.28	3.60E-07	99.28
30.0	60.0	8.13E-08	99.32	1.28E-07	99.03	1.28E-07	99.03
60.0	90.0	1.56E-08	99.20	3.73E-08	99.29	3.73E-08	99.29
90.0	60.0	3.30E-08	99.25	7.14E-08	99.09	7.14E-08	99.09
60.0	30.0	8.34E-08	99.06	1.97E-07	99.22	1.97E-07	99.22
30.0	0.0	5.52E-08	99.10	1.74E-07	99.34	1.74E-07	99.34

Table 1c. Diffusion coefficient values for the NR-112 sample.

Previous RH%	Target RH%	30 °C		50 °C		70 °C	
		Diffusion Coeff. (cm²/s)	R-sq. (%)	Diffusion Coeff. (cm²/s)	R-sq. (%)	Diffusion Coeff. (cm²/s)	R-sq. (%)
0.0	30.0	2.95E-07	100.00	3.90E-07	99.22	3.99E-07	99.17
30.0	60.0	1.11E-07	99.28	1.59E-07	99.24	1.71E-07	99.27
60.0	90.0	1.81E-08	99.16	4.91E-08	99.14	1.70E-07	99.48
90.0	60.0	4.18E-08	99.16	9.80E-08	99.06	2.17E-07	99.51
60.0	30.0	9.39E-08	99.19	2.46E-07	99.25	3.83E-07	99.04
30.0	0.0	6.26E-08	99.30	1.81E-07	99.02	2.64E-07	99.27

and 6. Figure 5 compares the diffusion constants for the N-117 (red), N-112 (blue) and NR-112 (green) samples grouped at each temperature: 30 °C (a.), 50 °C (b.), and 70 °C (c.). Similarly, Figure 6 contrasts the diffusion constants at 30 °C (red), 50 °C (blue), and 70 °C (green) grouped by each sample: N-117 (a.), N-112 (b.), and NR-112 (c.).
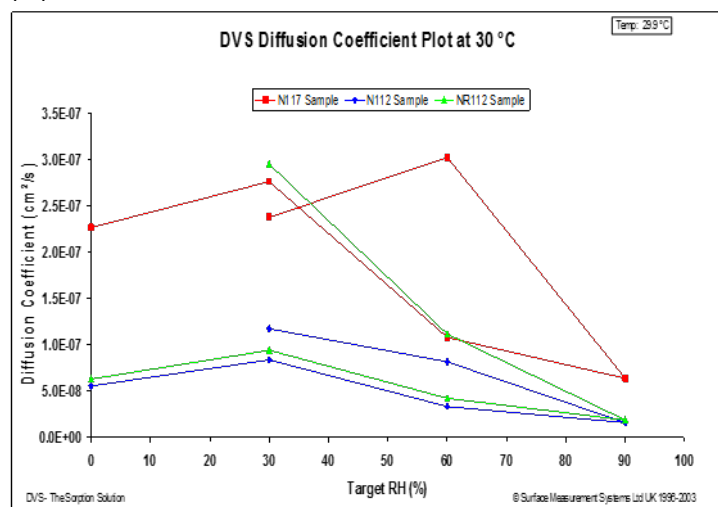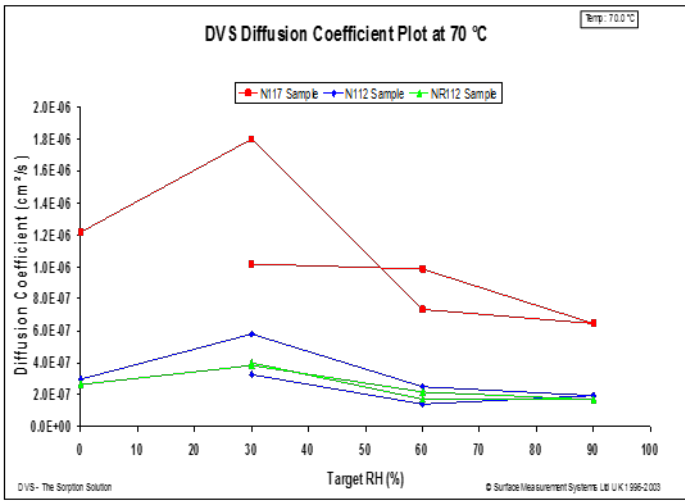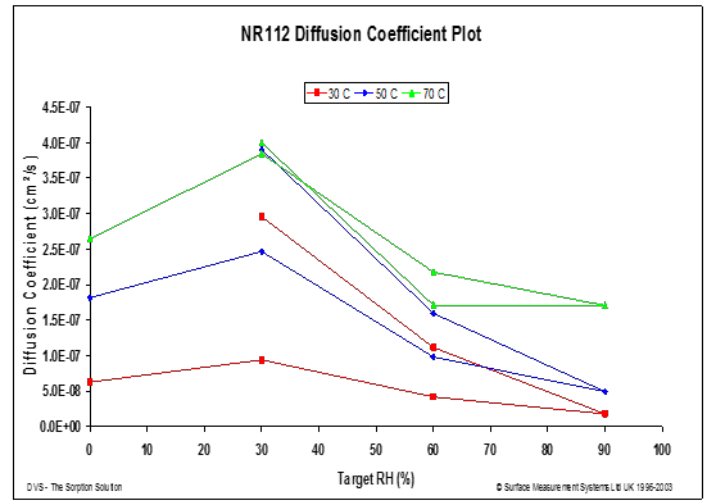

(a.)
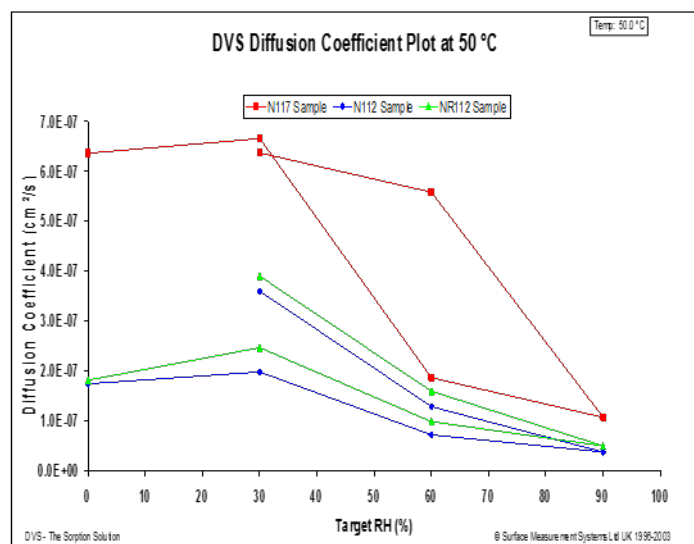
(b.)

To compare the results, the diffusion constants are displayed graphically in Figures 5

(c.)

Figure 5. Diffusion coefficients for the N-117 (red), N-112 (blue), and NR-112 (green) samples at 30 °C (a.), 50 °C (b.), and 70 °C (c.).

(c.)

Figure 6. Diffusion coefficients at 30 ° C (red), 50 °C (blue), and 70 °C (green) for the N-117 (a.), N-112 (b.), and NR-112 (c.) samples.

In general, the diffusion constants increase with temperature for each sample, as displayed in Figures 6a through 6c. This is most likely due to the increased molecular mobility within the sample at higher temperatures, which in turn facilitates water vapour diffusion into the bulk of the film. Also, during the sorption phase the diffusion constants decrease as the starting humidity increases. At higher starting humidity values, the sample is partially saturated with water. Therefore, there is a smaller water vapour concentration gradient between the sample and the surrounding air resulting in a smaller driving force for diffusion and lower diffusion coefficients. In comparing the N-117 and N-112 samples (see Figures 5a through 5c), the thicker N-117 sample generally has higher diffusion constants. In comparing the N-112 and NR-112 samples (Figures 5a through 5c), the dispersion-cast NR-112 sample generally has a slightly higher diffusion coefficient than the extruded N-112 sample.
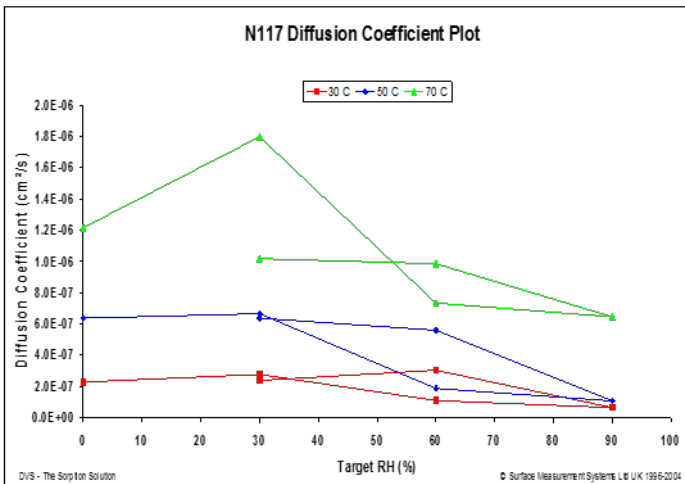
(a.)
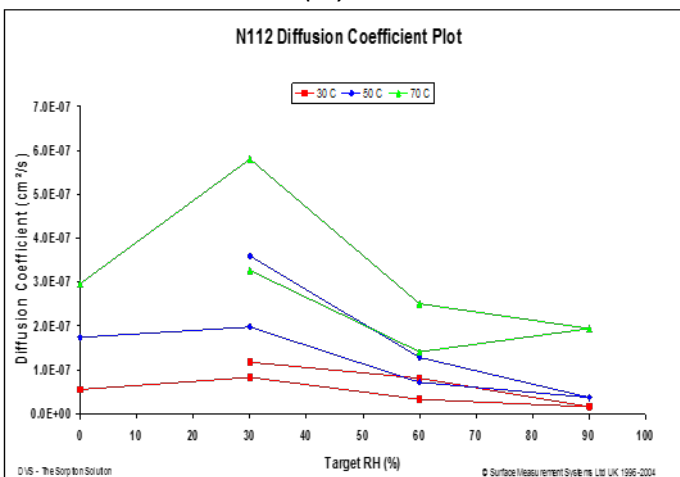
(b.)

Conclusion

Water sorption isotherms and diffusion coefficients were measured on three Nafion® based films over a range of temperatures. Multiple sorption/desorption isotherms indicated that water sorption was completely reversible and there was no sample history with respect to sorbed water. Increased temperatures lead to increased water sorption capacity and increased diffusion coefficients. The thicker N-117 sample had a lower percentage uptake than the thinner N-112 sample, most likely due to diffusion limitations. The extruded N-112 sample had a slightly higher percentage uptake compared to the dispersion cast NR-112 sample. Similar experiments could be performed on a range of fuel cell membrane materials to optimize chemical formulation and geometry of the films and to study gas diffusion layer moisture isotherms.

References

[1] Choi, P. and Datta, R., J. Electrochem. Soc. **150** (2003) E601.
[2] Nguyen, T.V. and Vanderborgh, N., J Membrane Sci. **143** (1998) 235.
[3] Lee, W-k, Shimpalee, S., and Van Zee, J.W., J Electrochem. Soc. **150** (2003) A341.
[4] Zawodzinski, T.A., Neman, M., Sillerud, L.O., and Gottesfeld, S., J. Phys. Chem. **95** (1991) 6040.
[5] Yang, C., Srinivasan, S., Bocarsly, A.B., Tulyani, S., and Benziger, J.B., J. Membrane Sci. **237** (2004) 145.
[6] Damay, F. and Klein, L.C., Solid State Ionics **162-163** (2003) 261.
[7] Savadogo, O., J. New Mater: Electrochem. Syst. **1** (1998) 47.
[8] Rivin, D., Meermeier, G., Schneider, N.S., Vishnyakov, A., and Neimarck, A.V., J. Phys. Chem. B **108** (2004) 8900.
[9] Legras, M., Hirata, Y., Nguyen, Q.T., Langevin, D., and Metayer, M., Desalination **147** (2002) 351.
[10] Levoguer, C.L. and Booth, J. SMS Application Note 16: Calculation of Diffusion Constants in Thin Polymer Films using DVS.